J. Chem. Sci. (2019) 131:86
https://doi.org/10.1007/s12039-019-1651-4

REGULAR ARTICLE

Coupling of CH_3OH and CO_2 with 2-cyanopyridine for enhanced yields of dimethyl carbonate over ZnO–CeO_2 catalyst

PRATHAP CHALLA[a,b], VENKATA RAO M[b], NAGAIAH P[b], NAGU A[a,b], DAVID RAJU B[a,b] and RAMA RAO K S[a,b,*]

[a]CSIR- Academy of Scientific and Innovative Research (CSIR-AcSIR), New Delhi, India
[b]Catalysis and Fine Chemicals Department, CSIR-Indian Institute of Chemical Technology, Hyderabad, Telangana 500 007, India
E-mail: ksramaraoiict@gmail.com

MS received 2 March 2019; revised 20 May 2019; accepted 21 May 2019

Abstract. The present work is aimed to produce dimethyl carbonate by coupling of CH_3OH and CO_2 with 2-cyanopyridine over ZnO–CeO_2 catalysts prepared by co-precipitation method. These catalysts were characterized by XRD, TEM, UV-Vis DRS, BET surface area, CO_2 and NH_3-TPD techniques and applied for the titled reaction. Among the investigated catalysts 10ZnO–90CeO_2 catalyst with CeO_2 crystallite size 8.0 nm exhibited 96% conversion of methanol with 99% selectivity to dimethyl carbonate. The superior catalytic activity is a unified effect of crystalline size of CeO_2 and presence of an optimum number of acidic and basic sites. This protocol offers enhanced conversion of methanol with the simultaneous conversion of 2-cyanopyridine into 2-picolinamide by removing water molecules formed in the reaction.

Keywords. Dimethyl carbonate; methanol; carbon dioxide; 2-cyano pyridine; acid-base property.

1. Introduction

Dimethyl carbonate (DMC) has been considered as a green chemical because it is projected as the substituent for toxic and corrosive chemicals like dimethyl sulfate and phosgene which are used as carbonylation and methylation agents respectively in organic synthesis.[1] Apart from that, DMC is a good solvent and a fuel additive. Because of its high dielectric constant, DMC is used as an electrolyte in lithium batteries.[2] The existence of high amount of oxygen in DMC and its low toxic and biodegradable nature makes it as a suitable replacement of methyl tert.butyl ether (MTBE), a gasoline oxygenate. It also acts as a promising octane booster.[3,4] Among the greenhouse gases, CO_2 is the main contributor. So, the utilization of CO_2 is very important. Availability of CO_2 in surplus quantity at cheap cost, hence it can be utilized as a precursor for synthesis of various chemicals and chemical intermediates.[5] Dimethyl carbonate (DMC) is one such an important chemical derived from CO_2.

There are so many routes to synthesize dimethyl carbonate. Among these, the production of DMC by combining methanol and carbon dioxide on a proper catalyst (Scheme 1) has been represented as a green chemical process.[6] Because of the thermodynamic constraints, the reaction between methanol and CO_2 results in low yields of DMC. However, higher pressure and instant removal of water produced by employing suitable dehydrating agents can shift the equilibrium towards products side.[7] However CO_2 is kinetically inert and thermodynamically stable. Hence, CO_2 activation is the key problem in its conversion to DMC.[8] The reaction between CH_3OH and CO_2 is slightly exothermic, with the heat of reaction of 23 kJ/mol. Hence to reach a higher amount of DMC yields, a lower reaction temperature is preferable. The low yields of DMC due to the generation of H_2O as a by-product.[9] Currently, CeO_2, ZrO_2,[10] CeO_2-ZrO_2,[11] K_2CO_3,[12] Cu-Ni/SBA-15, Nb_2O_5/CeO_2, Cu-Ni/graphite,[13] metal tetra alkoxides, $H_3PW_{12}O_{40}/ZrO_2$[14] are some of the major catalyst compositions for DMC synthesis. Among the heterogeneous catalysts, ZrO_2-based and CeO_2-based catalysts exhibit highest activities. Ki *et al.,* reported that CeO_2-ZnO catalysts are active in the synthesis of DMC from methanol and CO_2.[6] However, the conversion of methanol in their study is limited to 1% only and also there are no results regarding the

*For correspondence

Published online: 29 August 2019

influence of reaction temperature, pressure on the synthesis of DMC from methanol and CO_2. Since the synthesis of DMC from methanol and CO_2 is equilibrium controlled reaction, the removal of water is pre-requisite for the enhanced yield of DMC. Under pressurized reaction conditions, the mechanical removal of water is so difficult that the addition of dehydrating agent which doesn't disturb the targeted reaction is desirable. In this context, the addition of 2-cyanopyridine to the reaction would be an added advantage where 2-cyanopyridine converted to 2-picolinamide (an industrially interested chemical) by consuming the water molecules. Here some extent of methanol is reacted with 2-picolinamide to form methyl picolinate as described in Scheme 4. With these preliminary understandings, the present work has been undertaken to (i) apply ZnO-CeO_2 mixed oxide catalysts for the synthesis of dimethyl carbonate with high yield by coupling methanol and CO_2 reaction with the hydration of 2-cyanopyridine (Schemes 1, 2, 3) and optimizing reaction parameters for the best yield (ii) to establish a correlation between the catalytic activity and the characterization results.

The synthesis of DMC from methanol and CO_2 requires a catalyst with acidic and basic sites. The mechanism for the synthesis of DMC from CH_3OH and CO_2 over the acid-base catalyst is shown in Scheme 5.[15] Both the basic sites and acidic sites play a key role in the activation of methanol to methoxy species and methyl species respectively. Basic sites adsorb CO_2 and adsorbed CO_2 attacks on methoxy group to get methoxy carbonate anion. The reaction between methoxy carbonate anion with methyl species results in the formation of DMC.

Scheme 1. Direct synthesis of DMC from CO_2 and methanol.

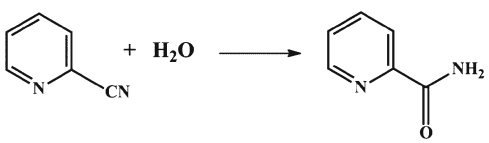

Scheme 2. Hydration of 2-cyanopyridine to 2-picolinamide.

2. Experimental

2.1 *Catalyst preparation*

ZnO-CeO_2 mixed oxide catalysts were prepared by the co-precipitation method. In a typical procedure, an aqueous solution of $(NH_4)_2Ce(NO_3)_6$ and $Zn(NO_3)_2$ was co-precipitated with (5%) aqueous NH_4OH solution at pH maintained at around 9–9.5. The resulting precipitate after ageing for 24 h was subsequently filtered with deionized water, washed several times until the pH of the filtrate become neutral. The resulting solid was dried in an oven at 100 °C for 12 h followed by calcination at 773 K for 5 h in static air. In the same manner, pure CeO_2 and ZnO were prepared by precipitation method. Finally, obtained catalysts named as (a) pure CeO_2 (b) 10wt%ZnO-90wt%CeO_2 (c) 30wt%ZnO-70wt%CeO_2 (d) 50wt%ZnO- 50wt%CeO_2 (e) 70wt%ZnO-30wt%CeO_2 (f) 90wt%ZnO-10wt%CeO_2 (g) Pure ZnO.

2.2 *Catalyst characterization*

The X-ray powder diffraction (XRD) patterns of the CeO_2 samples were recorded on Ultima-IV X-ray diffractometer (M/s. Rigaku Corporation, Japan) with Cu Ka radiation operated at 40 kV and 20 mA. The diffraction patterns were recorded in the 2θ range of 10–80° at a scan rate of 4°/min. The average crystallite size (D) was calculated using the Scherrer equation:

$$D = k\lambda / \beta \cos\theta$$

Where λ is X-ray wavelength, K constant of proportionality taken as 0.94, β is the full width at half maximum of the maximum intensity peak and θ is the diffraction angle. The BET surface areas of all catalysts were determined by nitrogen adsorption on an Autosorb Instrument (M/s. Quantachrome, USA). UV-Vis diffused reflectance spectra was recorded on a UV Win Lab spectrometer (M/s. Perkin Elmer, Germany) with an integrating sphere reflectance accessory in a range of 200–800 nm. The acidic and basic strengths of the samples were obtained by subjecting the catalyst sample

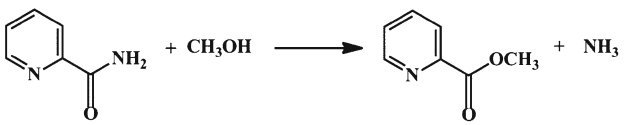

Scheme 4. Reaction of methanol with 2-picolinamide to form methyl picolinate.

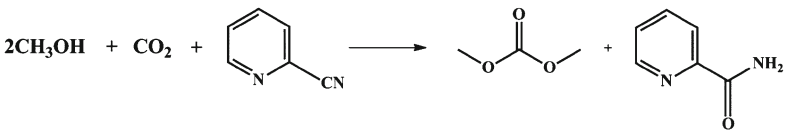

Scheme 3. Coupling of methanol and 2-cyanopyridine.

Mechanism

$CH_3OH \longrightarrow CH_3O^- + H^+$ (Over basic sites)

$CO_2 \longrightarrow CO_2^*$ (Over basic sites)

$CH_3O^- + CO_2^* \longrightarrow CH_3OCO_2^-$ (Over basic sites)

$CH_3OH \longrightarrow CH_3^+ + OH^-$ (Over acidic sites)

$CH_3OCO_2^- + CH_3^+ \longrightarrow CH_3O-\overset{\overset{O}{\|}}{C}-OCH_3$

(From basic sites) (From acidic sites)

Scheme 5. Mechanism for the synthesis of DMC from CH_3OH and CO_2 over acid-base catalyst.[16]

to the temperature-programmed desorption of NH_3 and CO_2 respectively on an Auto chem 2010 instrument (M/s. Micromeritics Instruments, USA). A sample of 0.25 g was placed in a U shaped quartz tube. The catalyst was activated by drying under helium flow (20 mL/min) followed by adsorption of CO_2 or NH_3 gas at 373 K for 30 min. The desorption of CO_2 or NH_3 takes place from 373 K to 873 K at a heating rate of 10 K/min.

2.3 *Catalytic activity*

The synthesis of DMC from CO_2 and CH_3OH was conducted in a pressure autoclave reactor over ZnO-CeO_2 catalyst. The reaction was coupled with hydration of 2-cyanopyridine. A stoichiometric amount of methanol (100 mmol), CO_2 (70 mmol), 2-cyanopyridine (50 mmol) and 0.6 g of ZnO-CeO_2 catalyst were charged into the reactor. The reactor was purged with CO_2 and pressurized to 4 MPa and then heated to a temperature of 393 K. After the completion of the reaction, the reactor was cooled to room temperature and depressurized. The reaction mixture was analyzed on a gas chromatograph, GC-17A (M/s. Shimadzu Instruments, Japan) equipped with flame ionization detector and OV-1 capillary column (30 m length, 0.53 mm id) and the product components were confirmed by GCMS, QP 5050 (M/s. Shimadzu Instruments, Japan).

3. Results and Discussion

3.1 *X-ray diffraction analysis*

Figure 1 shows the XRD patterns of (a) ZnO (b) 90Z-10C (C) 70Z-30C (d) 50Z-50C (e) 30Z-70C (f) 10Z-90C (g) CeO_2 catalysts. CeO_2 exhibited diffraction peaks due to the fluorite phase, while ZnO showed the characteristic diffraction peaks for the wurtzite phase. In the XRD patterns of ZnO-CeO_2 catalysts, the diffraction peaks at 2θ values of 31.7, 34.4, 36.2 and 63° corresponding to ZnO and the diffraction peaks at 2θ values of 28.7 and 33.2° corresponds to CeO_2. Furthermore, a mixed-phase of CeO_2 and ZnO was observed with 2θ values of 47.6 and 56.4°, which are in good agreement with the reported results.[16] The crystalline size of CeO_2 in ZnO-CeO_2 catalysts & BET surface area of catalysts are

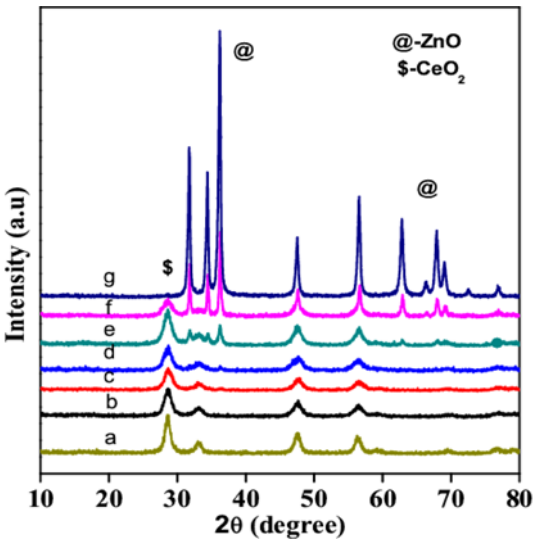

Figure 1. XRD of (a) Pure CeO_2, (b) 10Z-90C, (c) 30Z-70C, (d) 50Z-50C, (e) 70Z-30C, (f) 90Z-10C and (g) Pure ZnO catalysts.

Table 1. Textural features of CeO_2, ZnO and ZnO-CeO_2 catalysts.

Catalyst	Crystallite size (nm)[a]	Surface area (m^2/g)
CeO_2	7.1	76.0
10Z-90C	8.0	71.2
30Z-70C	10.2	60.8
50Z-50C	11.4	48.2
70Z-30C	18.6	37.2
90Z-10C	25.2	23.4
ZnO	54.2	8.9

[a]Crystallite sizes of CeO_2 are measured using Scherrer equation from (111) plane at $2\theta = 33.7°$ and for pure ZnO from the diffraction peak at $2\theta = 36.2°$.

illustrated in Table 1. In the XRD patterns of ZnO-CeO_2 catalysts, up to 50 wt % loading of ZnO, there are no significant peaks representing ZnO. Hence, the ZnO over CeO_2 exists either in amorphous form or in crystalline form with below the detection limit of the instrument. However, at higher loadings of ZnO on CeO_2 surface, high intense ZnO peaks were observed due to high crystalline nature of ZnO. Moreover higher ZnO loading is not good to well disperse on the surface of CeO_2. As well as the mutual interface between Ce and Zn oxide particles results in an increase in the surface areas with decreased crystalline sizes in the catalysts.

3.2 *BET surface analysis*

The BET-surface areas of the pure ZnO, pure CeO_2 and ZnO/CeO_2 (10Z-90C, 30Z-70C, 50Z-50C, 70Z-30Cand 90Z-10C) catalysts were shown in Table 1. Among all the synthesized catalysts, 10Z-90C, 30Z-70C were found to possess the highest BET surface area of 71.2 m^2/g, and 60.8 m^2/g respectively. With the increase in ZnO content from 10 wt% to 90 wt% the surface area of ZnO-CeO_2 catalysts decreases. It was majorly due to ceria species significantly facilitating enough space for the homogeneous dispersion of ZnO species accordingly high surface emerged in all catalysts. But high ZnO content in the catalysts play a negative role in view of the formation of agglomerated particles on the surface of the catalysts, which is responsible for less surface area and high crystalline size depicted in Table 1. It was further investigated from XRD patterns, high-intensity peaks observed in 90Z-10C catalyst rather than mild intensity peaks in the 10Z-90C catalyst. For that reason, 10Z-90C catalyst possesses the highest surface area of 71.2 m^2/g, whereas 90Z-10C presents the lowest surface area of only 23.4 m^2/g. Therefore, the highest surface area in the 10Z-90C catalyst was provided by uniform dispersion of zinc oxide particles on the surface of ceria species. It is noticed that there is a good correlation between the total adsorption capacity of CO_2, NH_3 and specific surface area of the catalysts.

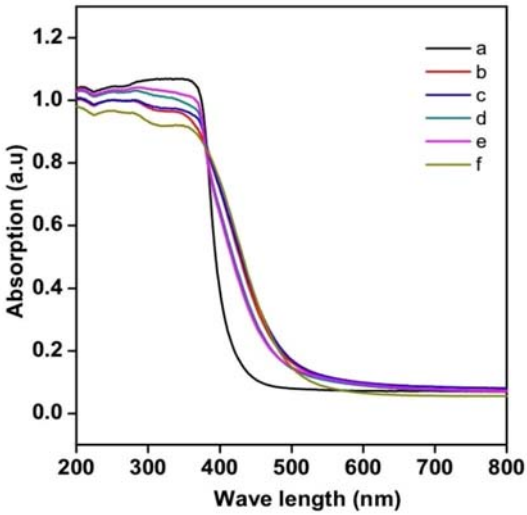

Figure 2. UV-Vis DRS patterns of (a) Pure CeO_2, (b) Pure ZnO, (c) 10Z-90C, (d) 30Z-70C, (e) 50Z-50C and (f) 70Z-30C catalysts.

Table 2. Band gap energies calculated from Tauc Plot method.

Catalyst	Band gap (eV)
CeO_2	2.74
10Z-90C	2.81
30Z-70C	2.82
50Z-50C	2.85
70Z-30C	2.94
ZnO	3.11

3.3 *UV-Vis-DRS studies*

The UV-Vis DRS patterns of CeO_2 and ZnO-CeO_2 catalyst were depicted in Figure 2. From this study, it is found that a signal at 280 nm in the pattern of pure CeO_2 and ZnO-CeO_2 is due to the intrinsic character of CeO_2 [17] while absorption edge at 413 nm in CeO_2 is blue-shifted for ZnO-CeO_2 mixed oxides which may be due to the presence of solid solution between Ce-O-Zn. The absorption bands at 256 and 296 nm are due to charge transfer transitions of $O^{2-} \rightarrow Ce^{3+}$ and $O^{2-} \rightarrow Ce^{4+}$.[18] Addition of CeO_2 to ZnO changes the absorption features indicating bands at 230, 280 and 340 nm in the UV region of the spectra due to localized transitions. Such narrow bands are reported in the spectra of ultrafine alignment of CeO_2 particles in SiO_2 and Al_2O_3 matrices.[19,20] The bandgap energy from UV-Vis DRS spectra was calculated using the Tauc plot method and presented

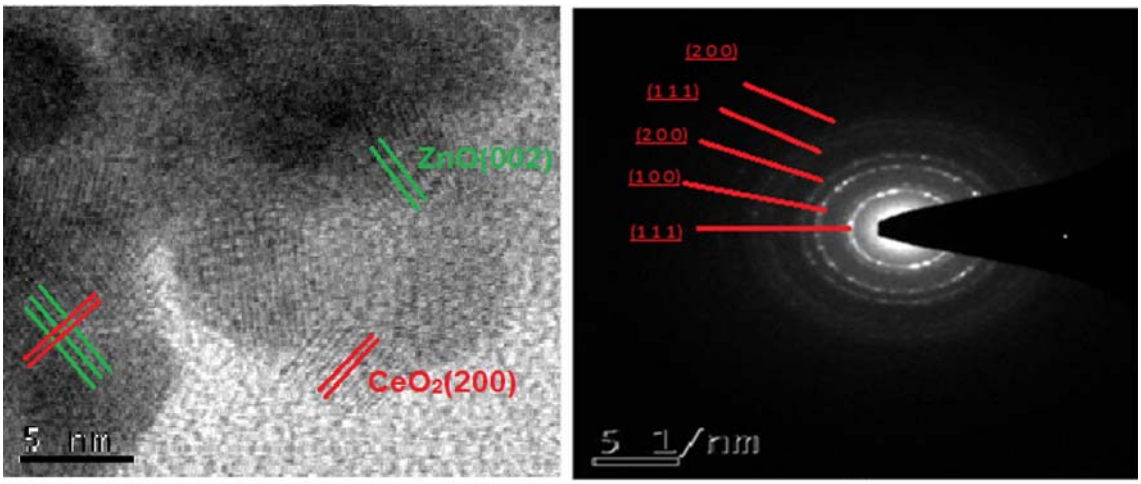

Figure 3. (a) TEM, (b) SAED images of 10Z- 90C catalyst indicates the circular planes which correspond to the existed peaks in the XRD patterns.

in Table 2. The band gap energy is increased from 2.74 eV to 2.94 eV with doping of ZnO to CeO_2. It means, with a decrease in CeO_2 content the band gap energy is increased. For pure ZnO, the band gap energy is 3.11 eV. The increase in band gap energies resulted in a decrease in surface oxygen vacancies.[21]

3.4 *Transmission electron spectroscopy (TEM)*

TEM studies were performed on 10Z-90C catalyst. The representative images were displayed in Figure 3. The HR-TEM and selected-area electron diffraction (SAED) patterns further confirmed the structure of the desired solid oxide materials. The HR-TEM image in Figure 3(a) clearly shows an interface between CeO_2 and ZnO species. The *d*-spacing values were calculated on the basis of the HR-TEM image. The planes existed in SAED image are in correlation with peaks in XRD patterns in Figure 1, and reported studies.[22,23] The calculated *d*-spacing values show that the ZnO species exhibited a hexagonal structure and that CeO_2 exhibited a cubic structure which is close agreement with the XRD results.

3.5 *Temperature programmed reduction studies*

The redox properties of the ZnO-CeO_2 catalysts were evaluated by temperature-programmed reduction (H_2-TPR). Figure 4 depicts the H_2-TPR profiles of the ZnO-CeO_2 catalysts. As we know that cerium can exist as Ce^{3+} and Ce^{4+} ions while zinc exists as Zn^{+2} only. Thereby CeO_2 has high oxygen storage capacity and possesses a larger number of oxygen vacancies.[24] In case of pure CeO_2 catalyst typically two reduction peaks are observed. The low-temperature peak is ascribed the most easily removable surface capping oxygen of CeO_2, while the high-temperature signal is caused by the removal of bulk oxygen. The H_2-TPR profiles of the mixed oxides ZnO-CeO_2 catalysts show a main broad reduction in the region between 763–833 K with different T_{max} values. For pure CeO_2, two reduction peaks at around 853 and 923 K were observed, which ascribed to the reduction of surface and bulk oxygen of CeO_2 respectively. It was interesting to note that two reduction peaks at 769 and 833 K of the ZnO-CeO_2 mixed oxide shifted to lower temperatures extremely relative to those of pure CeO_2. It was due to effective synergistic interface between ceria and zinc oxide species consequently exhibited higher catalytic activity than pure CeO_2 and ZnO catalysts, which is reliable with the H_2-TPR results.[25] It is due to the beneficial interactions between ceria and zinc leads to facial reduction properties of mixed oxide catalyst rather than individual oxides. Moreover, some extent of ZnO particles might be inserted into the CeO_2 lattice, these properties make the better catalytic activity.

3.6 *X-ray photoelectron spectroscopy studies*

The XPS analysis spectrum is shown in Figure 5. The ZnO-CeO_2 surface is composed of Zn, Ce, O, and C. The binding-energy values at 1021.61 eV and 1044.61 eV represent Zn $2p_{3/2}$ and Zn $2p_{1/2}$ in the ZnO-CeO_2 mixed oxide catalyst as shown in Figure 5.[23] The labels used in identifying Ce 3d XPS peaks were established by Burroughs *et al.*,[26] where V and U indicate the spin-orbit coupling $3d_{5/2}$ and $3d_{3/2}$, respectively. The peaks corresponding to V, V″, V‴, U, U″, U‴ represent the

presence of Ce^{4+}, whereas the peaks V_0, V′, U_0, U′ represent Ce^{3+} ions.[27] As shown in the figure, the Ce 3d spectrum is integrated to subsequent peaks at about 881 (V_0), 882.3 (V), 888.9 (V″), 897.5 (V‴), 899 (U_0), 901.2 (U), 907.0(U″), and 918 eV (U‴). The primary peaks of $3d_{5/2}$ and $3d_{3/2}$ are located at 882.3 and 901.2 eV, respectively. The peak V″ is the satellite peak arising from ionization of Ce $3d_{5/2}$, while the signals U″ and U‴ are accounting for ionization of Ce $3d_{3/2}$.[28] The satellite peak U‴ associated to the Ce $3d_{3/2}$ is a characteristic aspect hinting to the presence of tetravalent Ce ions in ceria compounds which is in good agreement with literature reports.[29]

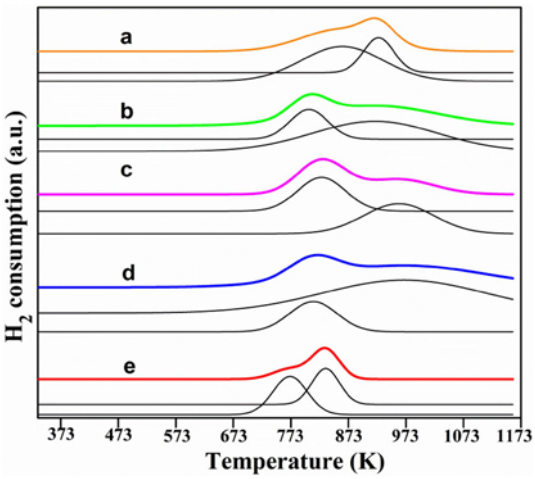

Figure 4. TPR patterns of (a) pure CeO_2, (b) 70Z-30C, (c) 50Z-50C, (d) 30Z-70C and (e) 10Z-90C.

3.7 *Temperature programmed desorption (TPD) of NH3*

Figure 6 shows the NH_3 -TPD profiles of the catalysts. The synthesis of DMC from CH_3OH and CO_2 involves the activation of CH_3OH to CH_3^+ species on the acidic sites of the catalyst. So, higher acidity of the catalyst is helpful to get more yield of DMC. During the reaction, the decomposition of CH_3OH molecule is higher on 10Z-90C catalyst due to the higher amount of acidic sites present in ZnO along with a small fraction of acidic sites in CeO_2. Among these catalysts, 10Z-90C possesses a higher amount of acidic sites which could be responsible for the better catalytic performance with respect to higher production of DMC from CH_3OH and CO_2. The acidity of the catalysts increased as the content of CeO_2 increased, whereas the acidity decreased at an excessive amount of CeO_2 content. Cerium oxide is more

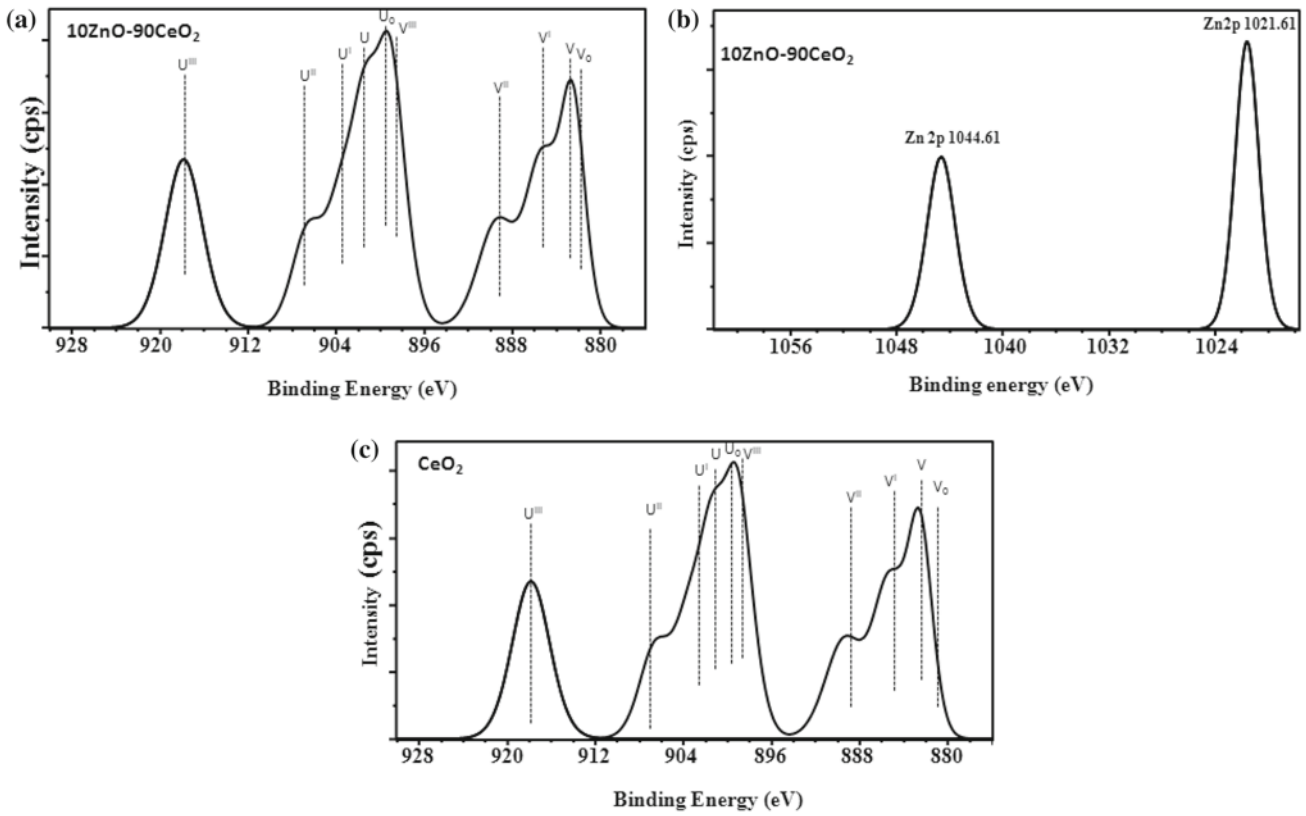

Figure 5. XPS spectra of (a) Ce 3d in 10Z-90C, (b) Zn 2p in 10Z-90C and (c) Ce 3d in pure CeO_2 samples calcined at 773K.

Table 3. The total acidity and basicity of the catalysts.

Catalyst	Number of acidic sites (mmol/g)	Acidic site density ($\times 10^{-2}$ mmol/m^2)	Number of basic sites (mmol/g)	Basic site density ($\times 10^{-2}$ mmol/m^2)
CeO_2	0.56	0.73	1.497	1.96
10Z-90C	0.75	1.1	1.775	2.49
30Z-70C	0.59	1.0	1.635	2.68
50Z-50C	0.51	1.05	1.322	2.74
70Z-30C	0.47	1.26	1.183	3.18
90Z-10C	0.37	1.58	0.666	2.84
ZnO	0.19	2.13	0.379	4.25

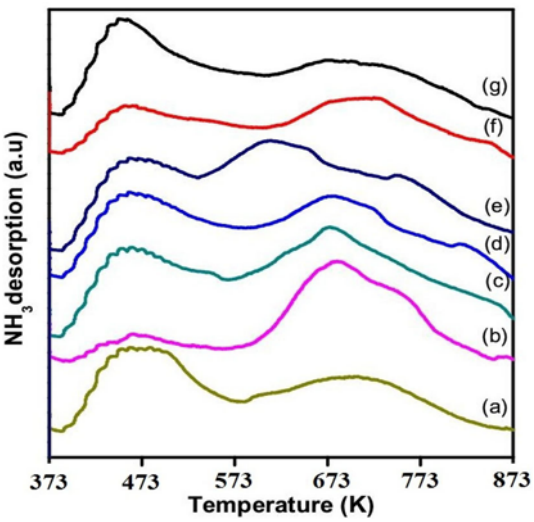

Figure 6. Temperature programmed desorption (TPD) patterns of NH_3: (a) pure CeO_2, (b) 10Z-90C, (c) 30Z-70C, (d) 50Z-50C, (e) 70Z-30C, (f) 90Z-10C and (g) pure ZnO.

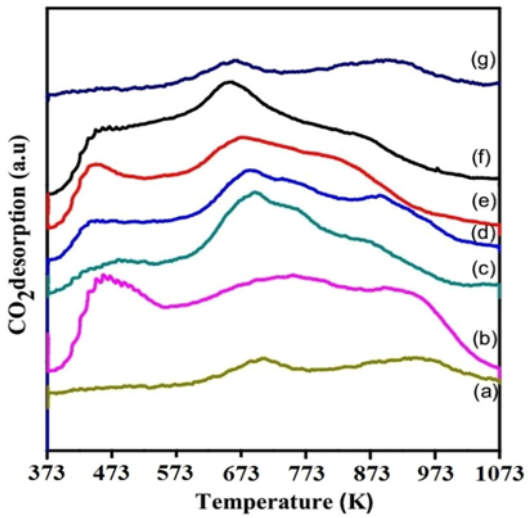

Figure 7. Temperature programmed desorption (TPD) patterns of CO_2: (a) pure ZnO, (b) 10Z-90C, (c) 70Z-30C, (d) pure CeO_2, (e) 30Z-70C, (f) 50Z-50C and (g) 90Z-10C.

basic oxide and therefore, a high amount of CeO_2 in the catalyst may result in a decrease of ammonia adsorption. In the present study based on catalytic activity, we assumed that there might be the considerable synergetic interface between Lewis acidity of ZnO and Lewis basicity of CH_3OH. The amount of acidity of catalysts calculated from NH_3-TPD peak area is summarized in Table 3.

3.8 *Temperature programmed desorption (TPD) of CO_2*

Not only acidic sites but also basic sites of the catalyst can also play an important role in the synthesis of DMC. Basic sites of the catalyst are more accountable for the formation of methoxy carbonate through a reaction between methoxy species and CO_2 molecules. Figure 7 shows the CO_2-TPD profiles of different catalysts. Among these catalysts, 10Zn-90C possesses more number of basic sites which could be useful in yielding better catalytic activity towards the synthesis of DMC from CH_3OH and CO_2. The introduction of an appropriate amount of Ce into ZnO could increase the number of basic sites in the catalyst, whereas an excessive amount of Ce could lead to a decrease in the amount of basic sites. The reduction in the amount of basic sites may be due to the aggregation of CeO_2 particles. It was reported that the CeO_2 species were exhibited better O_2 storage and releasing capacity which leads to adsorption of more number of CO_2 molecules in view of higher number of methoxy carbonate molecule formation during the reaction.[30] On 10Z-90C catalyst, we speculate that there could be better synergetic interactions between CeO_2 and CO_2 molecules which lead to the better conversion of CH_3OH molecules. Basicity of catalysts obtained from CO_2-TPD is described in Table 3. As can be seen from Scheme 5, both acidic and basic sites are major responsible for the better catalytic activity. Thus the amount of DMC obtained could be proportional to the high concentration of acidic and basic sites of

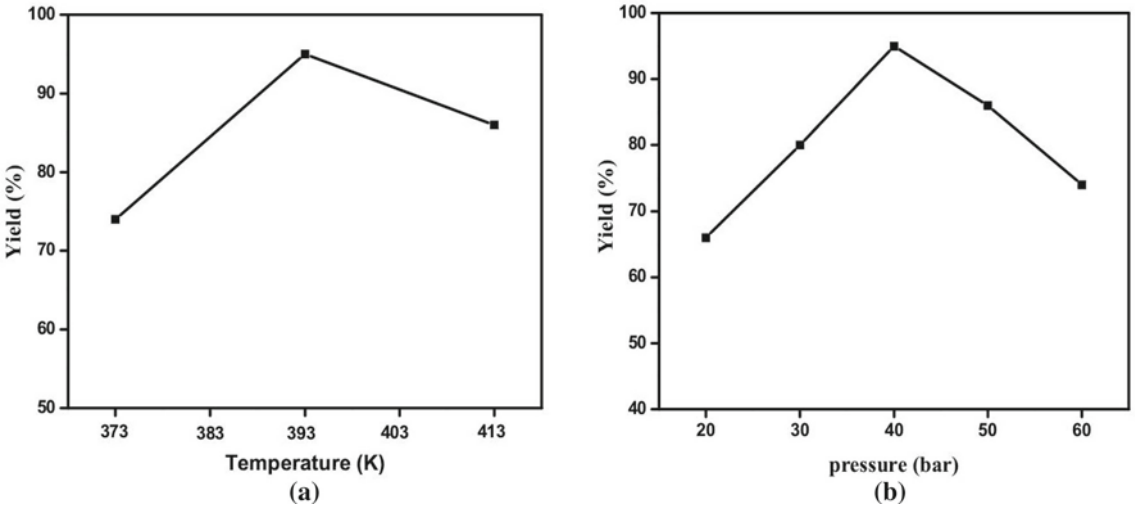

Figure 8. (a) Effect of reaction temperature (b) CO_2 Pressure on the DMC yield over 10Z-90C catalyst after 12 h catalytic reaction. Reaction conditions: Catalyst amount: 0.6 g, Methanol: 100 mmol, 2-cyanopyridine: 50 mmol.

the catalysts. Based on Figures 6 and 7, DMC yields are typically depends on more number of acidic and basic sites of the catalysts, which are close correlation with CO_2 and NH_3 TPD analysis shown in Figures 6 and 7. The surface acidic/basic site densities of the catalysts were calculated and presented in Table 3. The surface acidic site densities are increased from 0.73 x 10^{-2} mmol/m^2 (for pure CeO_2) to 1.58 $\times 10^{-2}$ mmol/m^2 (for 90Z-10C) with increase in ZnO loading. The surface basic site densities are also followed the same trend as surface acidic site density (1.96 x10^{-2} mmol/m^2 (for pure CeO_2) to 2.84 x10^{-2} mmol/m^2 (for 90Z-10C)). These results indicate that, the incorporation of ZnO in CeO_2 enhances the available surface acidic and basic sites per unit surface area of the catalyst.

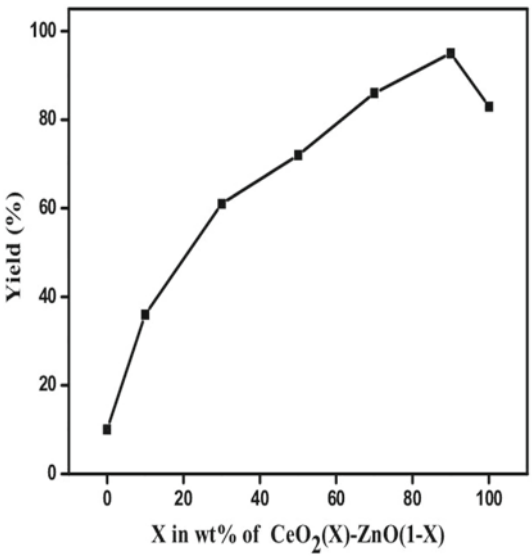

Figure 9. Catalytic performance of ZnO–CeO_2 mixed oxide catalysts. Reaction conditions: Catalyst amount: 0.6 g, Methanol: 100 mmol, 2-cyanopyridine: 50 mmol, Reaction temperature: 393 K, Pressure: 40 bar.

3.9 *Activity studies*

3.9a *Effect of reaction temperature and pressure*: Even though DMC synthesis is slightly exothermic, the high reaction temperature is needed for the activation of CH_3OH and CO_2. However, the activity decreases beyond 393 K due to considerable CO_2 and CH_3OH desorption.[31] The selectivity to DMC also declines with an increase in temperature due to the decomposition of DMC (Figure 8 (a)). DME observed as a side product is due to the decomposition of dimethyl carbonate.[32] It can also be obtained from MeOH *via* intermolecular dehydration in the presence of an acid-base catalyst at high temperature but this is very low when compared to the decomposition of DMC. The yield and selectivity of DMC increase with increasing pressure up to 40 bar (Figure 8 (b)). There is a decrease in the yield of DMC over 40 bar due to the dilution effect.

3.9b *Effect of loading*: The amount of formation of DMC over CeO_2, ZnO and ZnO-CeO_2 mixed oxide catalytic systems was shown in Figure 9. It is found that ZnO catalyst exhibited lower activity (14% CH_3OH conversion) than that of CeO_2 (84% conversion of CH_3OH) even though both catalysts are exhibited similar higher selectivity to DMC. Catalysts with 10 and 30% ZnO exhibited higher activity than that of CeO_2. Among these two, 10Z-90C exhibited higher activity (96% CH_3OH

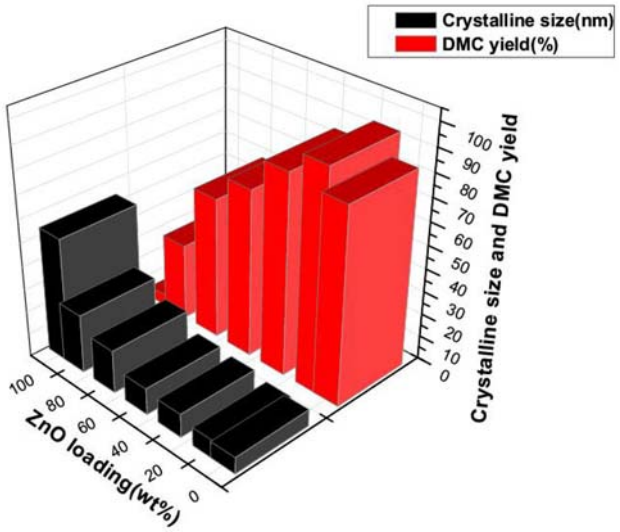

Figure 10. Loading of ZnO against the crystalline size of CeO_2 and DMC yield.

conversion with 99% selectivity to DMC) (Figure 9). Catalysts with higher ZnO content (>50%) showed lower activity when compared to bare CeO_2 because of high crystalline ZnO species existed on the surface of the CeO_2 leads to the mild surface area. CeO_2 - ZnO mixed oxide catalysts with more number of acidic and basic sites in the moderate region (ranging from 573–773 K temperature) showed enhanced catalytic activity.

From Figure 10, it is clear that the crystalline size of CeO_2 and as well as ZnO have a profound effect in governing the yield of DMC. The crystalline sizes of CeO_2 in ZnO-CeO_2 are increased with the incorporation of ZnO in CeO_2 and *vice versa*. In general, the catalytic activity is decreased at high crystalline sizes of metal oxides. In the present case, the best catalytic activity is obtained over the 10Z-90C catalyst with CeO_2 crystalline size of 8.0 nm even though the crystalline size of pure CeO_2 is 7.1 nm. It indicates that the catalytic activity of the catalyst can't be dependent alone on the crystalline size of CeO_2. In addition, the presence of surface acidic and basic sites is responsible for achieving the best yield of DMC. In particular, the optimum numbers of surface acidic and basic site densities along with small crystallites of CeO_2 are key contributors for the catalytic activity in the synthesis of DMC from CO_2 and methanol.

The reaction conditions for different catalysts used for the synthesis of DMC are reported in Table 4. Various catalysts have been reported for the synthesis of DMC from CO_2 and CH_3OH such as pure metal oxide, mixed metal oxides and bimetallic supported catalysts. Ahmed *et al.,* reported 7.6% CH_3OH conversion and 87% DMC selectivity over $Co_{1.5}PW_{12}O_{40}$ catalyst.[4] Over Cu-Ni/graphite, 10.2% CH_3OH conversion and 88% DMC selectivity were observed from the report of Bian *et al.*[14] Yingjie *et al.,* reported 5.3% CH_3OH conversion and 86% DMC selectivity over Cu–Fe/SiO_2 catalyst.[33] Qinghai *et al.,* reported 16.2% CH_3OH conversion and 100% DMC selectivity over CH_3OK catalyst.[34] Over Ce-Zr/Graphene, 58% of CH_3OH conversion and 57% of DMC selectivity were reported by Rim *et al.*[35] Over LG-HTO catalyst, 15.9% CH_3OH conversion and 99.9% DMC selectivity were observed from the report of Stoian *et al.*[32] Zhongwei *et al.,* reported 5.38% CH_3OH conversion and 83.1% DMC selectivity over $Ti_{0.04}Ce_{0.96}O_2$ catalyst.[36] 63% CH_3OH conversion and 97% DMC selectivity over

Table 4. Comparison of the activity of the present catalyst with the reported catalysts.

Catalyst	Temperature (K)	Pressure (bar)	CH_3OH Conversion (%)	DMC Selectivity (%)	References
$Co_{1.5}PW_{12}O_{40}$	473	1	7.6	87	4
Cu-Ni/graphite	383	12	10.2	88	14
LG-HTO	403	-	15.9	99.9	31
Cu-Fe/SiO_2	393	12	5.3	86	32
CH_3OK	353	73	16.2	100	33
Ce-Zr/Graphene	383	275	58	57	34
$Ti_{0.04}Ce_{0.96}O_2$	373	10	83.1	5.3	35
CeO_2-spindles	413	50	63	97	36
CeO_2	393	50	97	99	37
ZnO-CeO_2	443	70	<1	100	6
CeO_2-ZnO	393	40	2.7	100	This work
*CeO_2-ZnO	393	40	96	99	This work

* With addition of 2-cyanopyridine.

CeO_2 spindles were reported by Unnikrishnan *et al.*[37] Masayoshi *et al.,* reported 97% CH_3OH conversion and 99% DMC selectivity over CeO_2 catalyst for 16 h.[38]

In the present work, we report 96% conversion of methanol with 99% selectivity to DMC by coupling of methanol and CO_2 with 2-cyanopyridine. Since it is equilibrium controlled reaction, removal of H_2O, the by-product is necessary to get better methanol conversion. We achieved this, by coupling of CH_3OH with 2-cyanopyridine which can be beneficial to get more DMC yield. Hence coupling with 2-cyanopyridine has been used and afforded good activity results.

4. Conclusions

In conclusion, ZnO–CeO_2 catalysts prepared by co-precipitation method were found to be active in the synthesis of dimethyl carbonate *via* coupling of CH_3OH and CO_2 with 2-cyanopyridine. UV-Vis DRS patterns evidenced the formation of Ce-O-Zn solid solution. The synergetic interaction between ZnO and CeO_2 had improved the quantity of acidic and basic sites. Among the series of catalysts, 10ZnO–90CeO_2catalyst with CeO_2 crystallite size 8.0 nm and surface acid site density 1.1 x 10^{-2} mmol/m^2 and surface basic site density 2.49 x 10^{-2} mmol/m^2 delivered better results. Further, the addition of 2-cyanopyridine absorbed the formed water molecules during the reaction. Due to these unified effects, a maximum 95% yield of dimethyl carbonate was achieved at 393K.

References

1. Wang D, Zhang X, Ma J, Yu H, Shen J and Wei W 2016 La-modified mesoporous Mg-Al mixed oxides: effective and stable base catalysts for the synthesis of dimethyl carbonate from methyl carbamate and methanol *Catal. Sci. Technol.* **6** 1530
2. Praveen K, Vimal Chandra S and Indra Mani M 2015 Dimethyl carbonate synthesis via transesterification of propylene carbonate with methanol by ceria-zinc catalysts: role of catalyst support and reaction parameters *Korean J. Chem. Eng.* **32** 1774
3. Aouissi A, Abdullah Al-Othman Z and Al-Amro A 2010 Gas-phase synthesis of dimethyl carbonate from methanol and carbon dioxide over $Co_{1.5}PW_{12}O_{40}$ keggin-type heteropolyanion *Int. J. Mol. Sci.* **11** 1343
4. Lee H J, Park S, Kyu Song I and Chul Jung J 2011 Direct synthesis of dimethyl carbonate from methanol and carbon dioxide over $Ga_2O_3/Ce_{0.6}Zr_{0.4}O_2$ catalysts: Effect of acidity and basicity of the Catalysts *Catal. Lett*. **141** 531
5. Jun B, Min X, Shuanjin W, Xiaojin W, Yixin L and Yuezhong M 2009 Highly effective synthesis of dimethyl carbonate from methanol and carbon dioxide using a novel copper–nickel/graphite bimetallic nanocomposite catalyst *Chem. Eng. J.* **147** 287
6. Ki Hyuk K, Wangrae J, Chang Hoon L, Mieock K, Dong Baek K, Boknam J and In Kyu S 2013 Direct synthesis of dimethyl carbonate from methanol and carbon dioxide over $CeO_2(X)$–ZnO(1-X) nano-catalysts *J. Nanosci. Nanotechnol.* **13** 8116
7. Hye Jin L, Sunyoung P, Ji Chul J and In Kyu S 2011 Direct synthesis of dimethyl carbonate from methanol and carbon dioxide over $H_3PW_{12}O_{40}/Ce_XZr_{1-X}O_2$ catalysts: Effect of acidity of the catalysts *Korean J. Chem. Eng.* **28** 1518
8. Omae I 2006 Aspects of carbon dioxide utilization *Catal. Today* **115** 33
9. Masayoshi H, Masazumi T, Yoshinao N, Satoru S, Kimihito S, Ken-ichiro F and Keiichi T 2013 Ceria-catalyzed conversion of carbon dioxide into dimethyl carbonate with 2-cyanopyridine *ChemSusChem* **6** 1341
10. Jung K T and Bell A T 2001 An in situ infrared study of dimethyl carbonate synthesis from carbon dioxide and methanol over Zirconia *J. Catal.* **204** 339
11. Tomishige K and Kunimori K 2002 Catalytic and direct synthesis of dimethyl carbonate starting from carbon dioxide using CeO_2-ZrO_2 solid solution heterogeneous catalyst: effect of H_2O removal from the reaction system *Appl. Catal. A Gen*. **237** 103
12. Du M, Li Q, Dong W, Geng T and Jiang Y 2012 Synthesis of glycerol carbonate from glycerol and dimethyl carbonate catalyzed by K_2CO_3/MgO *Res. Chem. Intermed.* **38** 1069
13. Bian J, Xiao M, Wang S, Lu Y and Meng Y 2009 Graphite oxide as a novel host material of catalytically active Cu–Ni bimetallic nano particles *Catal. Commun.* **10** 1529
14. Jiang C, Guo Y, Wang C, Hu C, Wu Y and Wang E 2003 Direct synthesis of dimethyl carbonate from CO_2 and CH_3OH using 0.4 nm molecular sieves supported Cu-Ni bimetal catalyst *Appl. Catal. A Gen.* **256** 203
15. Praveen K, Patrick W, Vimal Chandra S, Roger G and Indra Mani M 2015 Dimethyl carbonate synthesis from carbon dioxide using ceria–zirconia catalysts prepared using a templating method: characterization, parametric optimization and chemical equilibrium modeling *J. Environ. Chem. Eng.* **3** 2943
16. Mishra B and Rao G 2006 Promoting effect of ceria on the physicochemical and catalytic properties of CeO_2–ZnO composite oxide catalysts *J. Mol. Catal. A - Chem.* **243** 204
17. Tighe C, Cabrera R, Gruar R and Darr J 2013 Scale up production of nanoparticles: continuous supercritical water synthesis of Ce–Zn oxides *Ind. Eng. Chem. Res.* **52** 5522
18. Bensalem A, Muller J C and Bozon-Verduraz F 1992 Faraday communications. From bulk CeO_2 to supported cerium–oxygen clusters: a diffuse reflectance approach *J. Chem. Soc., Faraday Trans.* **88** 153
19. Bensalem A, Bozon-Verduraz F, Delamar M and Bugli G 1995 Preparation and characterization of highly dispersed silica-supported ceria *Appl. Catal. A Gen.* **121** 81

20. Zaki M, Hussein G, Mansour S, Ismail H and Mekhemer G 1997 Ceria on silica and alumina catalysts: dispersion and surface acid-base properties as probed by X-ray diffractometry, UV–Vis diffuse reflectance and in situ IR absorption studies *Colloid Surf. A* **127** 47
21. Hongyan L, Fei Z, Yisong L, Guangyue W and Feng P 2013 Correlation of oxygen vacancy variations to bandgap changes in epitaxial ZnO thin films *Appl. Phys. Lett.* **102** 181908
22. Saravanan R, Mansoob Khan M, Gracia F, Qin J, Vinod Kumar G and Stephen A 2016 Ce^{3+}-ion-induced visible-light photocatalytic degradation and electrochemical activity of ZnO/CeO_2 nanocomposite *Sci. Rep.* **6** 31641
23. Saravanan R, Karthikeyan N, Govindan S, Narayanan V and Stephen A 2012 Photocatalytic degradation of organic dyes using ZnO/CeO_2 nanocomposite material under visible light *Adv. Mat. Res.* **584** 381
24. Iuliia P, Venkata Narayana K, Sebastian W and Andreas M 2015 Continuous synthesis of diethyl carbonate from ethanol and CO_2 over Ce-Zr-O catalysts *Catal. Sci. Technol.* **5** 2322
25. Tian-Yi M, Zhong-Yong Y and Jian-Liang C 2010 Hydrangea like Meso-macroporous ZnO-CeO_2 binary oxide materials synthesis, photocatalysis and CO oxidation *Eur. J. Inorg. Chem.* **2010** 716
26. Burroughs P, Hamnett A, Orchard A F and Thornton G 1976 Satellite structure in the *X*-ray photoelectron spectra of some binary and mixed oxides of lanthanum and cerium *J. Chem. Soc., Dalton Trans.* **17** 1686
27. Shingo W, Xiaoliang M and Chunshan S 2009 Characterization of structural and surface properties of nano crystalline TiO_2-CeO_2 mixed oxides by XRD, XPS, TPR, and TPD *J. Phys. Chem. C* **113** 14249
28. Benjaram M R, Komateedi N R and Pankaj B 2009 Copper promoted cobalt and nickel catalysts supported on ceria-alumina mixed oxide: Structural characterization and CO oxidation activity *Ind. Eng. Chem. Res.* **48** 8478
29. Beche E, Charvin P, Perarnau D, Abanades S and Flamant G 2008 Ce 3d XPS investigation of cerium oxides and mixed cerium oxide ($Ce_xTi_yO_z$) *Surf. Interface Anal.* **40** 264
30. Miki T, Ogawa T, Haneda M, Kakuta N, Ueno A, Tateishi S, Matsuura S and Sato M 1990 Enhanced oxygen storage capacity of cerium oxides in cerium dioxide/lanthanum sesqui oxide/alumina containing precious metals *J. Phys. Chem.* **94** 6464
31. Wu X, Xiao M, Meng Y and Lu Y 2006 Synthesis of copper-nickel/SBA-15 from rice husk ash catalyst for dimethyl carbonates production from methanol and carbon dioxide *J. Mol. Catal. A: Chem.* **249** 93
32. Stoian D, Taboada E, Llorca J, Molins E, Medina F and Segarra A 2013 Boosted CO_2 reaction with methanol to yield dimethyl carbonate over Mg-Al hydrotalcite - silicalyogels *Chem. Commun.* **49** 5489
33. Yingjie Z, Shuanjin W, Min X, Dongmei H, Yixin L and Yuezhong M 2012 Novel Cu–Fe bimetal catalyst for the formation of dimethyl carbonate from carbon dioxide and methanol *RSC Adv.* **2** 6831
34. Qinghai C, Chao J, Bin L, Hejin T and Yongkui S 2005 Structure of the active sites on H_3PO_4/ZrO_2 catalysts for dimethyl carbonate synthesis from methanol and carbon dioxide *Catal. Lett.* **103** 225
35. Rim S, Suela K, Tobias H, David M and Basudeb S 2015 Greener synthesis of dimethyl carbonate using a novel Ceria-zirconia oxide/Graphene nanocomposite catalyst *Appl. Catal. B-Environ.* **168** 353
36. Zhongwei F, Yunyun Z, Yuehong Y, Lizhen L, Min X, Dongmei H, Shuanjin W and Yuezhong M 2018 TiO_2-doped CeO_2 nanorod catalyst for direct conversion of CO_2 and CH_3OH to dimethyl carbonate: Catalytic performance and kinetic study *ACS Omega* **3** 198
37. Unnikrishnan P and Srinivas D 2016 Direct synthesis of dimethyl carbonate from CO_2 and methanol over CeO_2 catalysts of different morphologies *J. Chem. Sci.* **128** 6
38. Masayoshi H, Masazumi T, Yoshinao N, Kenji N, Kimihito S and Keiichi T 2014 Organic carbonate synthesis from CO_2 and alcohol over CeO_2 with 2-cyanopyridine: scope and mechanistic studies *J. Catal.* **318** 95